

# Expression profiling during ocular development identifies 2 *Nlz* genes with a critical role in optic fissure closure

Jacob D. Brown<sup>a,b</sup>, Sunit Dutta<sup>c</sup>, Kapil Bharti<sup>d</sup>, Robert F. Bonner<sup>e</sup>, Peter J. Munson<sup>f</sup>, Igor B. Dawid<sup>c,1</sup>, Amana L. Akhtar<sup>a</sup>, Ighovie F. Onojafe<sup>a</sup>, Ramakrishna P. Alur<sup>a</sup>, Jeffrey M. Gross<sup>g</sup>, J. Fielding Hejtmancik<sup>a</sup>, Xiaodong Jiao<sup>a</sup>, Wai-Yee Chan<sup>b,h</sup>, and Brian P. Brooks<sup>a,1</sup>

<sup>a</sup>Ophthalmic Genetics and Visual Function Branch, National Eye Institute, National Institutes of Health, Bethesda, MD 20892; <sup>b</sup>Biochemistry and Molecular & Cellular Biology, Georgetown University, 3900 Reservoir Road NW, Washington, DC 20007; <sup>c</sup>Laboratory of Molecular Genetics, <sup>e</sup>Section on Medical Biophysics, and <sup>f</sup>Section on Developmental Genetics, Eunice Kennedy Shriver National Institute of Child Health and Human Development, National Institutes of Health, Bethesda, MD 20892; <sup>d</sup>Mammalian Development Section, National Institute of Neurological Disorders and Stroke, National Institutes of Health, Bethesda, MD 20892; <sup>g</sup>Mathematical and Statistical Computing Laboratory, Center for Information Technology, National Institutes of Health, Bethesda, MD 20892; and <sup>h</sup>Molecular Cell & Developmental Biology, University of Texas at Austin, 1 University Station C1000, Austin, TX 78712-0195

Contributed by Igor B. Dawid, December 1, 2008 (sent for review August 4, 2008)

**The gene networks underlying closure of the optic fissure during vertebrate eye development are poorly understood. Here, we profile global gene expression during optic fissure closure using laser capture microdissected (LCM) tissue from the margins of the fissure. From these data, we identify a unique role for the C<sub>2</sub>H<sub>2</sub> zinc finger proteins *Nlz1* and *Nlz2* in normal fissure closure. Gene knockdown of *nlz1* and/or *nlz2* in zebrafish leads to a failure of the optic fissure to close, a phenotype which closely resembles that seen in human uveal coloboma. We also identify misregulation of *pax2* in the developing eye of morphant fish, suggesting that *Nlz1* and *Nlz2* act upstream of the *Pax2* pathway in directing proper closure of the optic fissure.**

coloboma | eye | pax2 | zinc finger protein | zebrafish

The mammalian eye begins as an evagination of forebrain neuroepithelium, the optic vesicle. As the optic vesicle approaches the surface ectoderm, it invaginates upon itself, forming a double-layered optic cup attached to the brain via the optic stalk. The asymmetric nature of this invagination leads to the formation of a gap along the ventral optic cup and optic stalk (the optic fissure) that remains open for hours to days, depending on the species. To form a spherical globe the margins of the optic fissure must meet and fuse ventrally during the 5th–7th weeks of gestation in humans (1).

Failure of optic fissure closure can lead to uveal coloboma, a malformation presenting as defects in the iris, ciliary body, retina, choroid, retinal pigment epithelium (RPE), and/or optic nerve in the inferonasal quadrant of the eye. The incidence of uveal coloboma in humans is between 0.5 and 2.6 per 10,000 births, depending on the population sampled, (2, 3) and may account for up to 10% of childhood blindness (4). Most cases of uveal coloboma are sporadic, although autosomal dominant, autosomal recessive, and X-linked modes of inheritance have been documented (5).

Numerous mutations in developmentally important genes are involved in human coloboma. Among these are *CHD7* (associated with CHARGE syndrome), *CHX10*, *GDF6*, *OTX2*, *PAX2*, *PAX6*, *SHH*, *SIX3*, *MAF*, *SOX2*, and *BMP4* (6–16) and many chromosomal aberrations. However, with the exception of *CHD7* in CHARGE syndrome, these mutations account for only a small subset of patients. The causes of the greater proportion of human colobomata remain unknown.

Given this complex and incomplete picture, we feel it is imperative to gain an increased understanding of the basic biology that governs normal closure of the optic fissure. Such an understanding will help inform a search for candidate genes of human disease. Toward this end we present here the results of

global expression profiling during optic fissure closure and identify *Nlz1* and *Nlz2* as critically important genes in this process.

## Results

**Optic Fissure Tissue Can Be Dissected Accurately and Consistently at Various Stages During Closure.** The different stages of the optic fissure can be clearly visualized by making sagittal sections through the mouse eye during early development, which represent the optic fissure at open (E10.5), closing (E11.5), and fused (E12.5) states (Fig. 1). Laser capture microdissection (LCM) was used to dissect tissue from the margins of the optic fissure consisting of the outer (presumptive RPE) and inner (presumptive neurosensory retina) layers of the retina. An approximately square-shaped block of optic fissure (50 × 50 μm) was dissected from each side of the fissure. Two rounds of linear amplification were performed on RNA isolated from each of the samples before microarray hybridization. In a pilot experiment, we found that 2 samples from E11.5 embryos that were isolated and hybridized on separate days had highly similar expression profiles ( $r = 0.997$ ), indicating minimal sample variation (supporting information (SI) Fig. S1).

**Identification of Temporally Regulated Transcripts as Candidate Genes for Controlling Closure.** Expression data were gathered in biological triplicate at E10.5, E11.5, and duplicate at E12.5. Each array represented pooled optic fissure tissue from 3 embryos from a single litter. Data analysis resulted in a subset of 250 probe sets that show variation with developmental time. These 250 probe sets represent 168 annotated genes and 54 hypothetical or predicted genes; 28 probe sets appeared more than once (Table S1). Temporal expression profile clustering shows substantial trends observed among the 250 probe sets (data not shown).

Author contributions: J.D.B., S.D., K.B., R.B., P.J.M., I.B.D., J.F.H., W.-Y.C., and B.P.B. designed research; J.D.B., S.D., K.B., R.B., A.L.A., I.F.O., R.P.A., X.J., and B.P.B. performed research; S.D., R.B., J.M.G., J.F.H., X.J., and W.-Y.C. contributed new reagents/analytic tools; J.D.B., K.B., P.J.M., I.B.D., and B.P.B. analyzed data; and J.D.B. and B.P.B. wrote the paper.

The authors declare no conflict of interest.

Freely available online through the PNAS open access option.

Data deposition: The data reported in this paper have been deposited in the Gene Expression Omnibus (GEO) database, www.ncbi.nlm.nih.gov/geo (accession no. GSE13103).

<sup>1</sup>To whom correspondence may be addressed. E-mail: dawidi@mail.nih.gov or brooks@nei.nih.gov.

This article contains supporting information online at [www.pnas.org/cgi/content/full/0812017106/DCSupplemental](http://www.pnas.org/cgi/content/full/0812017106/DCSupplemental).

© 2009 by The National Academy of Sciences of the USA

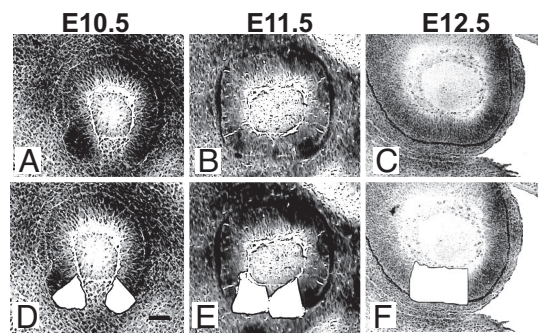


**Fig. 1.** Isolation of optic fissure tissue and experimental design. Representative sagittal sections through the eye of wild-type C57BL6/J mice at E10.5 (A and D), E11.5 (B and E), and E12.5 (C and F). Hematoxylin stained sections are seen before (A–C) and after (D–F) laser capture microdissection. Isolated tissue was used in expression profiling experiment. (Scale bar, 50  $\mu$ m.)

**Biological Filtering of Data.** To search for biological significance in the gene set, we inspected knockout/transgenic and expression databases (Mouse Genome Informatics, <http://www.informatics.jax.org>; VisiGene, <http://genome.ucsc.edu/cgi-bin/hgVisiGene>; Zfin, <http://zfin.org>). Of the 168 annotated genes, 49% (83/168) had been disrupted in mouse or zebrafish by targeted knockout, morpholino knockdown, or through random mutagenesis screens. Of these, 6% (5/83) were reported as having a coloboma, 26.5% (22/83) had another eye phenotype, 25.3% (21/83) had no reported eye phenotype; eye associations in 42.2% (35/83) could not be determined from published reports (Fig. S2). A high percentage of annotated genes from our screen were also confirmed to be expressed in the eye during the developmental stages assayed. Of the 46% (78/168) of genes for which in situ hybridization studies exist at relevant time points, 89.8% (70/78) are expressed in the eye, 5.1% (4/78) are not expressed in the eye, and the remaining 5.1% (4/78) are of undetermined expression in the eye.

**Real-Time PCR and in Situ Hybridization in Mouse Embryos Verifies Temporal and Spatial Gene Expression Patterns.** Several transcripts were selected for inclusion in further investigation on the basis of meeting 1 or more of the following criteria: they could be placed in a known developmentally regulated pathway, independent evidence of the trend in temporal expression, and/or expression in the eye, especially at the optic fissure. The expression profiles of 6 genes from our microarray analysis, which included the zinc finger protein encoding gene *Nlz2*, were validated by real-time PCR on independently dissected optic fissure tissue. A strong positive correlation was observed between expression profiles obtained by microarray analysis and real-time PCR in all cases (data not shown).

We also verified anatomic expression using in situ hybridization in whole mouse embryos and frozen sections. Strong expression was observed in the optic fissure for 5 of the gene products assayed and qualitative differences were noted among embryonic days E10.5, E11.5, and E12.5 (data not shown). Among the positive genes, we noted that transcripts encoding *Nlz2* are strongly expressed in the entire optic cup at E10.5. At E11.5, the time point we hypothesized was most critical to fusion, the *Nlz2* expression domain was confined to the closing optic fissure (Fig. S3E). Following fissure closure (E12.5), *Nlz* expression was undetectable.

**Two Related Zinc Finger-Containing Proteins, *Nlz1* and *Nlz2*, Are Each Necessary for Proper Optic Fissure Closure.** A morpholino knockdown strategy was used in zebrafish embryos to assess the functional significance of *nlz2* in optic fissure closure. Another

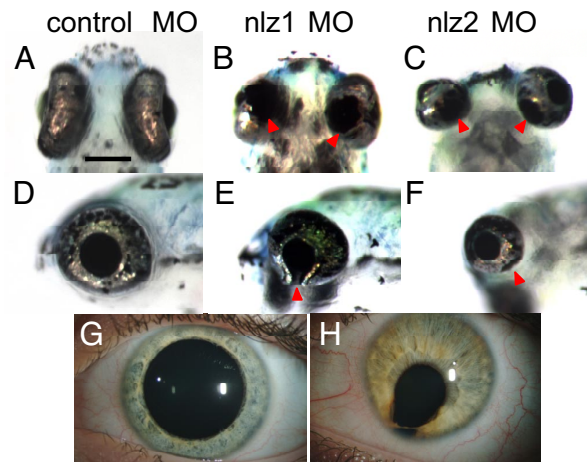


**Fig. 2.** Eye phenotype in *nlz1* and *nlz2* morphant zebrafish. At 5 dpf, fish injected with control MO show a completely fused optic fissure in the ventral eye (A, ventral; D, lateral) whereas there is an obvious coloboma in the ventral eye of the *nlz1* (B, ventral; E, lateral) and *nlz2* (C, ventral; F, lateral) morphant fish indicated by arrowheads. This phenotype recapitulates human uveal coloboma (H). Unaffected human eye (G). (Scale bar, 200  $\mu$ m.)

*Nlz* family member, *nlz1*, has also been identified in zebrafish (17) and both genes are expressed in the ventral eye at relevant developmental time points (see Fig. 4 H and I). The *Nlz* family has also been associated with molecules involved in eye development, including retinoic acid (RA), bone morphogenetic proteins (BMPs), and Pax2 (17, 18). We therefore reasoned that both *nlz1* and *nlz2* might play critical roles in fissure closure. To test this notion, morpholinos targeting the translation start site for both genes were injected into fertilized zebrafish eggs. The result was a marked delay in the apposition of the edges of the optic fissure beginning at 24 h postfertilization (hpf), a time when the optic fissure has begun to fuse in the control fish. At later time points, frank coloboma was observed in both *nlz1* and *nlz2* morphants (Fig. 2). However, whereas the eyes of *nlz1* morphants were close to normal in size (Fig. 2 B and E), the eyes of *nlz2* morphants were consistently microphthalmic (Fig. 2 C and F).

Histopathology in morphant fish at 5 and 6 dpf also reveals a striking failure of the optic fissure to fuse (Fig. 3 E, F, and H). Closure of the optic fissure can be clearly seen in control morpholino oligonucleotide (MO)-injected fish. At 6 dpf, the 2 margins of the optic fissure in *nlz1* morphants can be seen slipping past each other along the entry of the hyaloid vasculature in the ventral eye. Although retinal lamination—which is normally complete by this time—is largely normal in *nlz1* morphants, we do note small areas of retinal dysplasia/rosette formation (Fig. 3 E and H, arrows) and abnormal retinal vasculature (open arrowhead). By comparison, *nlz2* morphant eyes were smaller and had less well-defined retinal lamination (Fig. 3 C and F).

To confirm specificity, additional *nlz1* and *nlz2* morpholinos targeting the intron 1–exon 2 splice site were injected independently, resulting in the same phenotype as observed for the translation-blocking MOs. The optic fissure closure defect was observed in 102/103 *nlz1* morphant embryos using a translation start site blocking morpholino and 161/162 embryos using a splice site blocking morpholino. Similarly, in the case of *nlz2*, 64/66 fish had an optic fissure defect when injected with morpholino targeting the translation start site and 137/138 when the splice site was targeted. In a second series of injections, we established a grading scheme to score and quantify the severity of optic fissure defects seen in morphant fish, with grade 1 being

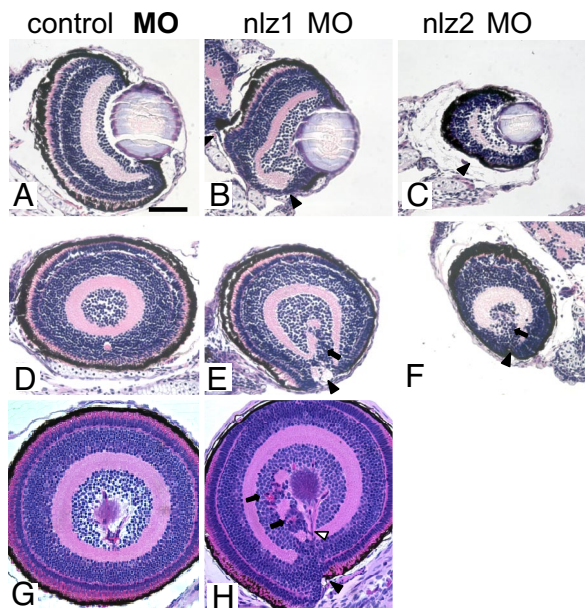


**Fig. 3.** Histopathology of *nlz* morphant fish. Coronal (A–C) and sagittal (D–H) planes through the zebrafish eye. Normal retinal lamination and a fused ventral fissure can be seen in control MO injected fish at 5 dpf (A and D) and at 6 dpf (G) (Top, dorsal; Bottom, ventral). Fissure closure defects can be seen in *nlz1* morphant fish at 5 dpf (B and E) and 6 dpf (H) and *nlz2* morphant fish at 5 dpf (C and F). The coloboma in morphant fish is accompanied by discontinuous RPE (black arrowhead), retinal dysplasia/rosettes (arrows), and abnormal vasculature (open arrowhead). H&E staining.

a fissure with a noticeable gap compared to control, grade 2 having a wider gap ( $20^{\circ}$ – $90^{\circ}$  gap as measured from the center of the lens), and grade 3 having the greatest gap ( $90^{\circ}$ – $170^{\circ}$ ) at 24 hpf (Fig. 4 A–F). The optic fissure closure defect is dose dependent because injecting 4 ng of *nlz1* MO or *nlz2* MO had a much less severe phenotype profile when compared to 8 ng (Fig. 4J). The coinjection of 4 ng *nlz1* and 4 ng *nlz2* MO, however, yields at least an additive effect. Coinjection of wild-type *nlz1* or *nlz2* mRNA with the respective *nlz* MO partially rescues the phenotype showing a greater percentage of normal fish and a less severe phenotype profile in general (Fig. 4J). In both splice-blocked morphants, correct morpholino targeting was confirmed using RT-PCR (Fig. S4).

***nlz1* and *nlz2* May Cause Coloboma by Misregulating *pax2.1* in the Optic Fissure.** The paired box transcription factors Pax2 and Pax6 have been shown to be 2 key regulators of optic stalk and optic cup identity, respectively (19, 20). In addition, homozygous disruptions or deletions of *Pax2* cause coloboma in mouse and zebrafish (21, 22). Given the importance of *Pax2* in optic fissure closure, we reasoned that Nlz1 and Nlz2 might affect a Pax2-dependent pathway in the developing eye. To test this hypothesis, we visualized *pax2.1* expression in zebrafish at 18 (Fig. 5 A–F) and 24 hpf (Fig. 5 G–L) using in situ hybridization in whole embryos. At 24 hpf, *pax2.1* is distinctly expressed in the optic stalk, closing fissure, midbrain/hindbrain boundary (MHB), and otic vesicle (Fig. 5 G and J). However, in *nlz1* knockdown embryos, *pax2.1* expression was almost completely absent from the lips of the closing optic fissure and stalk (Fig. 5 H and K). Interestingly, *nlz2* knockdown expanded the *pax2.1* expression domain in the eye from a ventral-anterior position in control fish at 18 hpf to nearly the entire optic vesicle (Fig. 5 C and F). The expansion is also pronounced at 24 hpf, laterally and dorsally into the inner layer of the developing retina (Fig. 5 I and L).

*pax6* is also strongly expressed in the eye and forebrain in

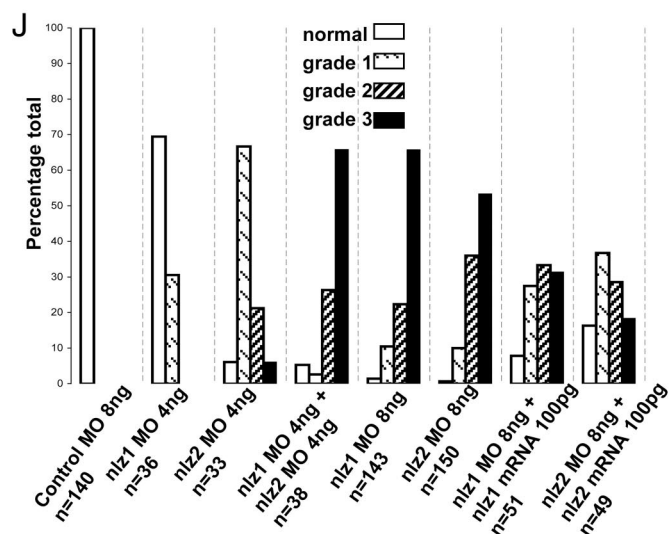
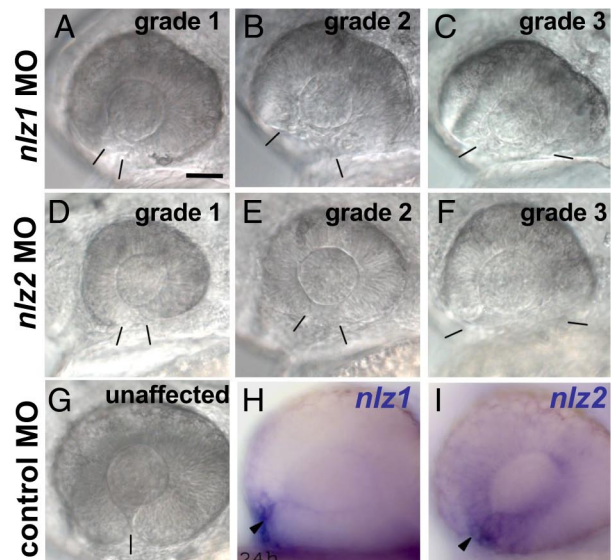


**Fig. 4.** Phenotypic grades of *nlz* morphant fish 24 hpf. *nlz1* MO (A–C) or *nlz2* MO (D–F) splice site MO injected fish were scored as having a grade 1 (A and D), grade 2 (B and E), or grade 3 (C and F) optic fissure defect. At 24 hpf, the margins of the optic fissure are apposed in normal eyes (G) and closure is just beginning. Bars delineate edges of optic fissure. (Scale bar, 50  $\mu$ m.) The results of the phenotype profiling are summarized in the bar graph (J) where lower grade closure defects are observed at low doses of either *nlz1* or *nlz2* MO, yet an effect which is at least additive is seen when these doses are combined. A higher dose of either morpholino produces strong optic fissure defects in morphant fish, which is partially rescued by coinjection of respective wild-type mRNA. Expression of *nlz1* (H) and *nlz2* (I) in wild-type zebrafish embryos at 24 hpf shows expression at the optic fissure (arrowheads).

zebrafish at 24 hpf (Fig. 5M). Because of the critical role of *pax6* in eye development we performed in situ hybridization to detect whether *nlz1* or *nlz2* knockdown affected the expression of this transcription factor. The expression domain of *pax6* in *nlz1* morphants was mildly expanded into the ventral optic cup at 24 hpf (Fig. 5N) and somewhat contracted in *nlz2* morphants (Fig. 5O).

We next chose to assay other markers of eye development to ascertain whether *nlz* knockdown was affecting *pax2.1* specifically or was causing a more global disruption of developmental regulation. *vax1* and *vax2* are well-characterized markers of the optic stalk and ventral retina and have also been shown to cause optic fissure defects when deficient in mouse and zebrafish





**Statistical Analysis of Microarray Data.** Normalized data were then analyzed in parallel in the statistical software JMP 6.0 (SAS, Cary, NC) and open-source scripts (MSCL toolbox, J. Barb and P. Munson, 2004; available at <http://abs.cit.nih.gov>). Filtering of the data included: (i) removing probes not present at at least 1 time point, (ii) setting a false discovery rate of <0.15, and (iii) setting a fold change of >2 over time as significant. Because Robust Multi-array (RMA) and S10 normalization and subsequent analysis resulted in 2 overlapping, but distinct sets of genes, we combined the 2 into 1 set of 168 unique, significantly regulated probes that represented genes present in 1 or both analyses without duplication.

**Probe Set Verification.** Reverse transcription was performed using cDNA Reverse Transcription kit (Applied Biosystems) according to manufacturer's protocol. Primer and TaqMan probe set Mm00520908.m1 was used for amplification and detection of *Nlz2* and reactions were normalized using mouse GAPDH predeveloped TaqMan primer/probe set (Applied Biosystems). Gene expression was visualized in wild-type C57BL/6J embryos using previously published protocol (37) using IMAGE clone 6401144 (Zfp503). Whole mount in situ hybridization in zebrafish was done as described previously (38).

**Morpholino Gene Knockdown and mRNA Rescue in Zebrafish.** Wild-type AB/TL zebrafish were injected at the 1–4 cell stage with 4–8 ng antisense morpholino oligos (Gene Tools, LLC), targeted to the translation start site or splice site of specific transcripts (39). Morpholino sequences were: 5' ATCCAGGAG-GCAGTTCGCTCATCTG 3', targeting translation start site of *nlz1*; 5' ATGGTT-TAGAAGTCGTACTCAATG 3', targeting *nlz1* intron 1–exon 2 splice boundary; 5' ACCCAATTCTCATGTATTTTGTGG3', targeting *nlz2* translation start site; 5' ATCGAGCTGCGAGAATAGATAAAAC3', targeting *nlz2* intron 1–exon 2 splice boundary. A standard control morpholino targeting human  $\beta$ -globin was used as a negative control. For RT-PCR, RNA from 20 whole embryos at 24 hpf injected with 8 ng *nlz1* or *nlz2* splice-site blocking morpholinos was

isolated using RNeasy Mini kit (Qiagen) and reverse transcribed using cDNA Reverse Transcription kit (Applied Biosystems). PCR was performed using intron spanning primers as previously published (18).

Full-length cDNA IMAGE clones 7405421 for *nlz1* and 2643152 for *nlz2* were obtained from Open Biosystems. The ORF of *nlz1* and *nlz2* was PCR amplified (primer sequences available upon request) and cloned into PCR II vector using TOPO TA cloning kit (Invitrogen), subsequently cut using *Clal* and *XbaI* and ligated into pCS2+ cut with the same enzymes. Clones were sequence verified. *pax2.1* in pCS2+ plasmid was a gift from Alexander Picker and was cut with *NotI*. Capped transcripts were made from these plasmids using mMACHINE in vitro transcription kit following manufacturer's protocol (Ambion). One hundred to 150 pg of these transcripts were then injected in embryos independently injected with 8 ng of *nlz1* or *nlz2* translation start site blocking morpholinos.

**PAX2 Promoter Studies.** For ChIP, ARPE19 cells were transfected with Flag-tagged constructs containing in-frame fusions of human *Nlz1* and *Nlz2* cDNAs. Cells were processed according to the recommendations in the protocol for ChIP IT Express kit (Active Motif) and ChIP was performed as described previously (40). See Fig. S5 for additional methods. Transactivation experiments were performed in ARPE19 cells using a standard protocol detailed in Fig. S6.

**ACKNOWLEDGMENTS.** The authors thank Abdel Elkalhoun of the National Human Genome Research Institute Microarray Core for his assistance with microarray processing and the National Eye Institute histology core. We thank A. Picker for the full-length *pax2.1* plasmid (University of Technology, Dresden, Germany). This research was supported by the Intramural Research Program of the National Eye Institute and Eunice Kennedy Shriver National Institute of Child Health and Human Development, National Institutes of Health. J.D.B. was partially supported by a stipend from the Georgetown University MD/PhD program.

1. O'Rahilly (1966) The early development of the eye in staged human embryos. *Contrib Embryol* XXXVIII(25–263):1–45.
2. Bermejo E, Martinez-Frias ML (1998) Congenital eye malformations: clinical-epidemiological analysis of 1,124,654 consecutive births in Spain. *Am J Med Genet* 75(5):497–504.
3. Porges Y, et al. (1992) Hereditary microphthalmia with colobomatous cyst. *Am J Ophthalmol* 114(1):30–34.
4. Maumenee IH, Mitchell TN (1990) Colobomatous malformations of the eye. *Trans Am Ophthalmol Soc* 88:123–132; discussion 133–125.
5. Traboulsi E (1999) Colobomatous microphthalmia, anophthalmia, and associated malformation syndromes. *Genetic Diseases of the Eye*, ed Traboulsi E (Oxford Univ Press, New York), pp 51–80.
6. Jamieson RV, et al. (2003) Pulverulent cataract with variably associated microcornea and iris coloboma in a MAF mutation family. *Br J Ophthalmol* 87(4):411–412.
7. Vissers LE, et al. (2004) Mutations in a new member of the chromodomain gene family cause CHARGE syndrome. *Nat Genet* 36(9):955–957.
8. Asai-Coakwell M, et al. (2007) GDF6, a novel locus for a spectrum of ocular developmental anomalies. *Am J Hum Genet* 80(2):306–315.
9. Ragge NK, et al. (2005) Heterozygous mutations of OTX2 cause severe ocular malformations. *Am J Hum Genet* 76(6):1008–1022.
10. Eccles MR, Schimmenti LA (1999) Renal-coloboma syndrome: a multi-system developmental disorder caused by PAX2 mutations. *Clin Genet* 56(1):1–9.
11. Azuma N, et al. (2003) Mutations of the PAX6 gene detected in patients with a variety of optic-nerve malformations. *Am J Hum Genet* 72(6):1565–1570.
12. Schimmenti LA, et al. (2003) Novel mutation in sonic hedgehog in non-syndromic colobomatous microphthalmia. *Am J Med Genet A* 116(3):215–221.
13. Wallis DE, et al. (1999) Mutations in the homeodomain of the human SIX3 gene cause holoprosencephaly. *Nat Genet* 22(2):196–198.
14. Ferda Percin E, et al. (2000) Human microphthalmia associated with mutations in the retinal homeobox gene CHX10. *Nat Genet* 25(4):397–401.
15. Wang P, Liang X, Yi J, Zhang Q (2008) Novel SOX2 mutation associated with ocular coloboma in a Chinese family. *Arch Ophthalmol* 126(5):709–713.
16. Bakrania P, et al. (2008) Mutations in BMP4 cause eye, brain, and digit developmental anomalies: overlap between the BMP4 and hedgehog signaling pathways. *Am J Hum Genet* 82(2):304–319.
17. Andreazzoli M, Broccoli V, Dawid IB (2001) Cloning and expression of noz1, a zebrafish zinc finger gene related to Drosophila noC. *Mech Dev* 104(1–2):117–120.
18. Hoyle J, Tang Y, Wiertel E, Wardle F, Sive H (2004) *nlz* gene family is required for hindbrain patterning in the zebrafish. *Dev Dyn* 229(4):835–846.
19. Schwarz M, et al. (2000) Spatial specification of mammalian eye territories by reciprocal transcriptional repression of Pax2 and Pax6. *Development* 127(20):4325–4334.
20. Ekker SC, et al. (1995) Patterning activities of vertebrate hedgehog proteins in the developing eye and brain. *Curr Biol* 5(8):944–955.
21. Torres M, Gomez-Pardo E, Gruss P (1996) Pax2 contributes to inner ear patterning and optic nerve trajectory. *Development* 122(11):3381–3391.
22. Lun K, Brand M (1998) A series of no isthmus (noi) alleles of the zebrafish *pax2.1* gene reveals multiple signaling events in development of the midbrain-hindbrain boundary. *Development* 125(16):3049–3062.
23. Bertuzzi S, Hindges R, Mui SH, O'Leary DD, Lemke G (1999) The homeodomain protein *vax1* is required for axon guidance and major tract formation in the developing forebrain. *Genes Dev* 13(23):3092–3105.
24. Barbieri AM, et al. (2002) *Vax2* inactivation in mouse determines alteration of the eye dorsal-ventral axis, misrouting of the optic fibres and eye coloboma. *Development* 129(3):805–813.
25. Mui SH, Kim JW, Lemke G, Bertuzzi S (2005) *Vax* genes ventralize the embryonic eye. *Genes Dev* 19(10):1249–1259.
26. Takeuchi M, Clarke JD, Wilson SW (2003) Hedgehog signalling maintains the optic stalk-retinal interface through the regulation of *Vax* gene activity. *Development* 130(5):955–968.
27. Iuchi S (2001) Three classes of C2H2 zinc finger proteins. *Cell Mol Life Sci* 58(4):625–635.
28. Runko A, Sagerstrom C (2004) Isolation of *nlz2* and characterization of essential domains in *Nlz* family proteins. *J Biol Chem* 279(12):11917–11925.
29. Schubert HD (2005) Structural organization of choroidal colobomas of young and adult patients and mechanism of retinal detachment. *Trans Am Ophthalmol Soc* 103:457–472.
30. Alvarez Y, et al. (2007) Genetic determinants of hyaloid and retinal vasculature in zebrafish. *BMC Dev Biol* 7:114.
31. Chang L, Blain D, Bertuzzi S, Brooks BP (2006) Uveal coloboma: clinical and basic science update. *Curr Opin Ophthalmol* 17(5):447–470.
32. Torres M, Gómez-Pardo E, Dressler G, Gruss P (1995) Pax-2 controls multiple steps of urogenital development. *Development* 121:4057–4065.
33. Macdonald R, et al. (1995) Midline signalling is required for Pax gene regulation and patterning of the eyes. *Development* 121(10):3267–3278.
34. Sehgal R, Karcavich R, Carlson S, Belecky-Adams TL (2008) Ectopic Pax2 expression in chick ventral optic cup phenocopies loss of Pax2 expression. *Dev Biol* 319(1):23–33.
35. Nakamura M, Choe SK, Runko AP, Gardner PD, Sagerstrom CG (2008) *Nlz1/Znf703* acts as a repressor of transcription. *BMC Dev Biol* 8(1):108.
36. Pedone PV, et al. (1996) The single Cys2-His2 zinc finger domain of the GAGA protein flanked by basic residues is sufficient for high-affinity specific DNA binding. *Proc Natl Acad Sci USA* 93(7):2822–2826.
37. Wilkinson D, Nieto M (1993) *Methods in Enzymology: Guide to Techniques in Mouse Development* (Academic, San Diego).
38. Toyama R, et al. (1995) The LIM class homeobox gene *lim5*: implied role in CNS patterning in *Xenopus* and zebrafish. *Dev Biol* 170(2):583–593.
39. Nasevicius A, Ekker SC (2000) Effective targeted gene 'knockdown' in zebrafish. *Nat Genet* 26(2):216–220.
40. Bharti K, Liu W, Csermely T, Bertuzzi S, Arnheiter H (2008) Alternative promoter use in eye development: the complex role and regulation of the transcription factor MITF. *Development* 135(6):1169–1178.